International Journal of Electrical, Electronic and Communication Sciences
ISSN: 2517-9438
Vol:11, No:3, 2017

Optimal Duty-Cycle Modulation Scheme for Analog-To-Digital Conversion Systems

G. Sonfack, J. Mbihi, B. Lonla Moffo

***Abstract*—**This paper presents an optimal duty-cycle modulation (ODCM) scheme for analog-to-digital conversion (ADC) systems. The overall ODCM-Based ADC problem is decoupled into optimal DCM and digital filtering sub-problems, while taking into account constraints of mutual design parameters between the two. Using a set of three lemmas and four morphological theorems, the ODCM sub-problem is modelled as a nonlinear cost function with nonlinear constraints. Then, a weighted least p^{th} norm of the error between ideal and predicted frequency responses is used as a cost function for the digital filtering sub-problem. In addition, MATLAB *fmincon* and MATLAB *iirlnorm* tools are used as optimal DCM and least p^{th} norm solvers respectively. Furthermore, the *virtual simulation* scheme of an overall prototyping ODCM-based ADC system is implemented and well tested with the help of Simulink tool according to relevant set of design data, i.e., 3 KHz of modulating bandwidth, 172 KHz of maximum modulation frequency and 25 MHZ of sampling frequency. Finally, the results obtained and presented show that the ODCM-based ADC achieves under 3 KHz of modulating bandwidth: 57 dBc of SINAD (signal-to-noise and distorsion), 58 dB of SFDR (Surpious free dynamic range) -80 dBc of THD (total harmonic distorsion), and 10 bits of minimum resolution. These performance levels appear to be a great challenge within the class of oversampling ADC topologies, with 2^{nd} order IIR (infinite impulse response) decimation filter.

***Keywords*—**Digital IIR filter, morphological lemmas and theorems, optimal DCM-based DAC, virtual simulation, weighted least p^{th} norm.

I. Introduction

THE oversampling ADC is widely encountered in programmable instrumentation systems. However, it could be implemented from different switching modulation techniques, e.g., sigma-delta modulation (SDM) [1], pulse-width modulation (PWM) [2], and duty-cycle modulation (DCM) [3]. The common principle of oversampling ADC techniques is illustrated in Fig. 1, where the input signal x is transformed into a switching periodic wave $x_m(x, t)$. Then, the resulting oversampled format x_m (x, kT), is processed by a *decimation* process, in order to build an accurate digital image of x to be used for decision making in a digital instrumentation context. However, the main drawbacks of a basic PWM-based ADC technique result from its open loop architecture, its greedy frequency spectrum and its architectural complexity. In the other side, the implementation of SDM technique leads to the complex building topology and to the lack of analytical models to be used for exact analysis and characterization. Furthermore, beside a number of technical limitations of PWM and SDM techniques, it has been shown that [4], [5] the DCM technique combines the merits of a robust closed loop topology, with known analytical characteristics. As an implication, the novelty of this paper relies on the challenge of modelling and solving oversampling ADC optimization problems, within the relevant and robust subclass of linear DCM policies.

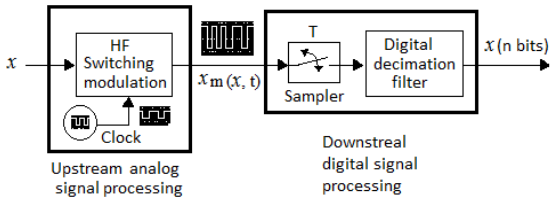

Fig. 1 Oversampling ADC principle

In Section II, the knowledge on the DCM-based ADC topology is outlined. Then, a decentralized optimal modulation scheme is presented in Section III, followed in Section IV by a case study of a prototyping ODCM-based ADC system. Then, the conclusion of the paper is presented in Section V.

II. DCM-Based ADC Topology

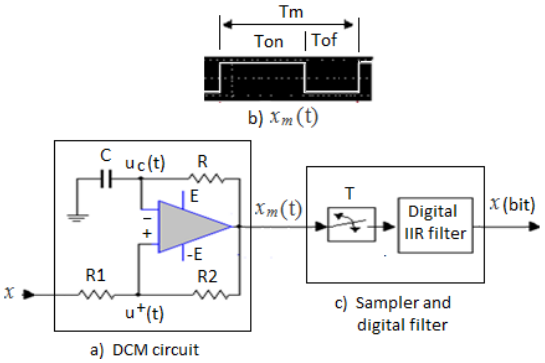

Fig. 2 DCM-Based ADC topology

This section outlines relevant characteristics, from which the optimization problem for DCM-based ADC topology will

G. Sonfack is a graduate Student in the PhD training program of the Faculty of Science of the University of Dschang (Cameoon). She is with the Electrical Department of Advanced Vocational Training Center of Douala, Cameroon (e-mail: beatricesonfack@gmail.com).

J. Mbihi is with the EEAT (Electrical, Electronics, Automatic and Telecommunication) research laboratory, University of Douala, Cameroon. He is also with the Department of Electrical and Electronics Engineering, at ENSET of the University of Douala, Cameroon (e-mail: mbihidr@yahoo.fr).

B. Lonla Moffo is with the EEAT (Electrical, Electronics, Automatic and Telecommunication) research laboratory of the University of Douala, Cameroon. He is also with the Department of Electrical and Electronics Engineering, at ENSET of the University of Buea (e-mail: moffolb@yahoo.fr).

be formulated in Section III. The basic DCM-based ADC topology shown in Fig. 2 consists of a simple upstream DCM circuit and a downstream digital *IIR* (infinite input response) with sampling period T.

The notations x, x_m (x, t), $T_{on}(x, \alpha)$, $T_{of}(x, \alpha)$, α stand for modulating input signal, modulated wave with time varying period $T_m(x, \alpha) = T_{on}(x, \alpha) + T_{of}(x, \alpha)$, pulse width time, switching downtime, and a design parameter, respectively.

Unlike complex input interfaces for PWM and SDM architectures, a DCM circuit is self-oscillating (no external clock source), and is equipped with positive and negative feedback loops, while offering a minimum hardware realization. These intrinsic findings are at the heart of its numerous merits as it will be detailed later. The parameters associated with the DCM circuit are given by (1):

$$\alpha = \alpha_1 = 1 - \alpha_2 = \frac{R_1}{R_1+R_2}, \tau = R\,C \tag{1}$$

Then, its dynamic behaviour is governed by the set of equations (2):

$$\begin{cases} u^+(t) = \alpha\ x_m(t) + (1-\alpha)x(t) & \text{(a)} \\ \varepsilon(t) = u^+(t) - u_C(t) & \text{(b)} \\ x_m(t) = E\ sign\left(\varepsilon(t)\right) & \text{(c)} \\ \dfrac{du_C(t)}{dt} = -\dfrac{1}{\tau}uc(t) + \dfrac{1}{\tau}x_m(t) & \text{(d)} \\ x(t) < E & \text{(e)} \end{cases} \tag{2}$$

A. Characteristics of DCM-Based ADC topology

The set of equations (3)-(12) summarizes the relevant analytical characteristics of the DCM-based topology. Most of these equations have been established or analysed in depth in previous research works [5]-[8].

1. Fourier series of $x_m(t, x, \alpha)$ [3]-[5]

$$x_m(t, x, \alpha) = (2R_m(x, \alpha) - 1)E + \frac{4E}{\pi}\sum_{n=1}^{\infty}\sin\left(\frac{n\pi R_m(x,\alpha)}{n}\right)\cos\frac{2\pi n t}{T_m(x)} \tag{3}$$

2. Pulse width time [3]

$$T_{on}(x, \alpha) = \tau\,\mathrm{Log}\left(\frac{(1-\alpha)x-(1+\alpha)E}{(1-\alpha)x+(\alpha-1)E}\right) \tag{4}$$

3. Pulse down time [3]

$$T_{off}(x, \alpha) = \tau\,\mathrm{Log}\left(\frac{(1-\alpha)x+(1+\alpha_1)E}{(1-\alpha)x-(\alpha-1)E}\right) \tag{5}$$

4. DCM time period [3]

$$T_m(x, \alpha) = \tau\,\mathrm{Log}\left(\frac{((1-\alpha)x)^2-((1+\alpha)E)^2}{((1-\alpha)x)^2-((\alpha-1)E)^2}\right) \tag{6}$$

5. DCM function [4]

$$D_m(x, \alpha) = \frac{T_{on}(x,\alpha)}{T_m(x,\alpha)} = \frac{\ln\left(\frac{(1-\alpha)x-(1+\alpha)E}{(1-\alpha)x+(\alpha-1)E}\right)}{\ln\left(\frac{((1-\alpha)x)^2-((1+\alpha)E)^2}{((1-\alpha)x)^2-((\alpha-1)E)^2}\right)} \tag{7}$$

6. Linear approximation of $D_m(x, \alpha)$ [3]

$$\widetilde{D}_m(x, \alpha) = \frac{\alpha\, x}{E(1+\alpha)\log\left(\frac{1+\alpha}{1-\alpha}\right)}x + \frac{1}{2} \tag{8}$$

7. Static gain of an analog DCM filter [5], [6]

$$K_a = \left(\frac{1+\alpha}{2\,\alpha}\right)\mathrm{Log}\left(\frac{1+\alpha}{1-\alpha}\right) \tag{9}$$

8. Discrete transfer function of the IIR filter [5], [6]

$$F(z) = \frac{b2\,z^2 + b1\,z + b0}{z^2 + a1\,z + a0} \tag{10}$$

9. Static gain of the digital IIR filter [4]-[8]

$$K_f = K_a = \frac{b2 + b1 + b0}{1 + a1 + a0} \tag{11}$$

10. Resolution (bits) [9], [10]

$$m(x, \alpha) = \log_2\left(\frac{f\,ech}{1/Tm(x,\alpha)}\right) \tag{12}$$

III. ODCM ADC TOPOLOGY

For a known modulating signal x, the goal of the optimization problem to be modelled and solved here is to find a set of critical parameters α in (1) and {b2, b1, b0, a1, a2} in (10), (11), which minimizes the overall DCM error between the modulating input x and its digital image to be produced at the output of the IIR filter.

Because of the serial processing structure of signals in a DCM topology, it is easier to resort to a decentralized optimization approach, i.e., to separately optimize the upstream DCM source and the downstream digital IIR filtering, while taking into account the equality constraint of static gains between the two as predicted by (9) and (11).

A. Optimization of the DCM Circuit

1) DCM Optimization Cost

Since the exact DCM function $D_m(x, \alpha)$ given by (7) is nonlinear, the extraction of the digital image of x from (7) given by $D_m(x, \alpha)$ using a downstream linear IIR solver, can be quite *accurate* through the linear range of $D_m(x, \alpha)$ as modelled by (8). In this case, the resulting linear approximation error incurred is given by (13):

$$|\varepsilon^*(x, \alpha)| = \left|D_m(x, \alpha) - \widetilde{D}_m(x, \alpha)\right| \tag{13}$$

In addition, a more suitable optimization cost function to be minimized under linear DCM approximation might arise from morphological Lemmas outlined below.

Lemma 1. For an arbitrary parameter α, the nonlinear DCM function $D_m(x, \alpha)$, modelled by (7) is increasingly monotonous in the modulating space.

Lemma 2. The nonlinear DCM function $D_m(x,\alpha)$ modelled by (7) is linear around a neighbourhood of the set point:

$$(x = 0, D_m(0, \alpha) = 1/2).$$

Lemma 3. The linear range of $D_m(x, \alpha)$, required for high accuracy and reliability is maximum if the slope $p_m(0, \alpha)$ observed in (8) is maximum.

The proofs of Lemmas 1 and Lemma 2 arise from numerical analysis results presented in Fig. 3 (a), where the increasing monotony and the local linearity properties around the set point ($x = 0$, $D_m(0, \alpha) = 1/2$), are quite apparent. In addition, Fig. 3 (b) shows the realistic nature of Lemma 3 since the range of the linear approximation error is an increasing function of the slop $p_m(x=0, \alpha) = \frac{\alpha}{E(1+\alpha)\,\mathrm{Log}\left(\frac{1+\alpha}{1-\alpha}\right)}$ in (8). As an implication, an equivalent cost function to be maximized for achieving minimum absolute linear approximation error is given by (14).

As an implication, an equivalent cost function to be maximized for achieving minimum absolute linear approximation error is given by (14):

$$p_m(\alpha) = \frac{\alpha}{E(1+\alpha)\,\mathrm{Log}\left(\frac{1+\alpha}{1-\alpha}\right)} \tag{14}$$

2) DCM Optimization Constraints

The first obvious constraint arising from (1) is given by:

$$0 < \alpha < 1 \tag{15}$$

In addition, the optimization cost function (14) is associated with constraints, resulting from three morphological Theorems.

Theorem 1. Monotony of $T_{on}(x, \alpha)$: The DCM pulse width time $T_{on}(x, \alpha)$ in (4) is a monotonous function of x and α over the composite range $|x| < E$ and $0 < \alpha < 1$.

Theorem 2. Monotony of $T_{of}(x, \alpha)$: The DCM pulse down time $T_{of}(x, \alpha)$ in (5), is a monotonous function of x and α, for $|x| < E$ and $0 < \alpha < 1$.

Theorem 3. Convexity of $T_m(x, \alpha)$: The DCM period $T_m(x, \alpha)$ in (6) (or the CM frequency $f_m(x, \alpha) = 1/T_m(x, \alpha)$ equivalently) is a convex function of x with minimum value (or maximum frequency $f_m(x, \alpha)$ equivalently) at $x = 0$, and behaves as the increasing branch of a convex function of α in the composite range $|x| < E$ and $0 < \alpha < 1$.

The proof of Theorem 1 relies on the analysis of the gradient (directional derivative) of $T_{on}(x, \alpha)$ in (4). The structure of this gradient presented in (16) shows that both terms $\frac{\partial T\mathrm{on}(x,\alpha)}{\partial x}$ and $\frac{\partial T\mathrm{on}(x,\alpha)}{\partial \alpha}$ are strictly positive for all x and α in the composite range $|x| < E$ and $0 < \alpha < 1$. Therefore, Theorem 1 is proven.

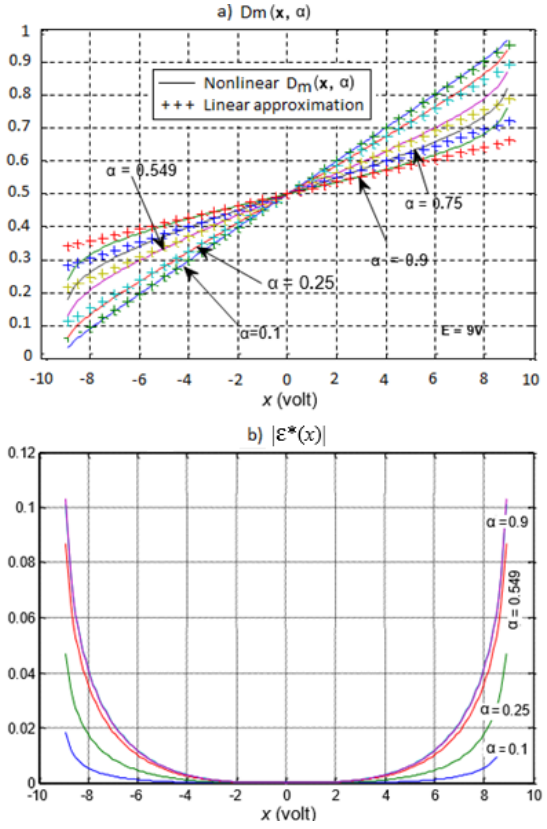

Fig. 3 Graphical analysis of $D_m(x, \alpha)$ and $|\varepsilon^*(x)$ [9] |

$$\begin{cases} \frac{\partial T\mathrm{on}(x,\alpha)}{\partial x} = \frac{2\,\tau\,E\,\alpha}{(E-x)\,(E-x+a(E+x)} \\ \frac{\partial T\mathrm{on}(x,\alpha)}{\partial \alpha} = \frac{2\,\tau\,E}{(1-\alpha)\,(E-x+a(E+x)} \end{cases} \tag{16}$$

The proof of Theorem 2 relies on a similar reasoning from (16), where it is obvious to observe that $\frac{\partial T\mathrm{of}(x,\alpha)}{\partial x}$ is strictly negative, whereas $\frac{\partial T\mathrm{of}(x,\alpha)}{\partial \alpha}$ is strictly positive over the range $|x| < E$ and $0 < \alpha < 1$. Hence, Theorem 2 is clearly proven also.

$$\begin{cases} \frac{\partial T\mathrm{of}(x,\alpha)}{\partial x} = \frac{-2\,\tau\,E\,\alpha}{(E+x)\,(E-x+a(E-x)} \\ \frac{\partial T\mathrm{of}(x,\alpha)}{\partial \alpha} = \frac{2\,\tau\,E}{(1-a)\,(E+x+a(E-x)} \end{cases} \tag{17}$$

On the other side, (17) is useful for the proof of Theorem 3. In fact, it is clear that $\frac{\partial T\mathrm{m}(x,\alpha)}{\partial x}$ in (17) is positive or negative if x is positive or negative, and 0 if $x = 0$. This finding is a proof of the convexity property $T_m(x, \alpha)$,

$$\begin{cases} \frac{\partial T\mathrm{m}(x,\alpha)}{\partial x} = \frac{8\,\tau\,E^2\,\frac{x}{(E^2-x^2)}}{(E^2-x^2)\,(1+a^2)+2\,a\,(E^2+x^2)} \\ \frac{\partial T\mathrm{m}(x,\alpha)}{\partial \alpha} = \frac{4\,\tau\,E^2\,\frac{(1+a)}{(1-a)}}{(E^2-x^2)\,(1+a^2)+2\,a\,(E^2+x^2)} \end{cases} \tag{18}$$

Furthermore, an unconstraint analysis of the sign of

$\frac{\partial Tm\,(x,\alpha)}{\partial \alpha}$ might predict ideally that $T_m\,(x, \alpha)$ appears to be a convex function of α with minimum at α = -1. However, since $0 < \alpha < 1$, it is clear that the realistic portion of $T_m\,(x, \alpha)$ is included into in the increasing branch of an ideal convex function. Thus, Theorem 3 is clearly proved also.

As an implication of Theorem 3, given a modulating bandwidth $[f_{min}\,(x_{max}\,, \alpha)\ f_{max}\,(0\,, \alpha)]$, the boundaries $f_{min}\,(x, \alpha) = 1/T_{max}\,(x, \alpha)$ and $f_{max}\,(0\,, \alpha)$ might be chosen according to the following analytical constraints:

$$\begin{cases} f_{max}(0\,,\alpha) = \frac{1}{2.\tau.\ln\left(\frac{\alpha+1}{1-\alpha_1}\right)} \\ f_{min}(x_{max},\alpha) = \\ \frac{1}{\tau.\ln\left(\frac{\left[((1-\alpha)\,x_{max})^2-((\alpha+1)E)^2\right]}{\left[((1-\alpha)\,x_{max})^2-((\alpha-1)E)^2\right]}\right)} \end{cases} \quad (19)$$

3) Mathematical Structure of the Optimal DCM Problem

As a summary of the analysis conducted in this section, the DCM optimization problem to be solved is formulated by (20). It consists structurally of a static nonlinear cost criteria (20 (a)), associated with a set of static nonlinear constraints (20 (b)-(d)).

$$\begin{cases} \alpha^* = \mathrm{Max}_\alpha \left(p_m(\alpha) = \frac{\alpha}{E(1+\alpha)\,\mathrm{Logn}\left(\frac{1+\alpha}{1-\alpha}\right)} \right) \text{(a)} \\ with \\ f_{m0}(\alpha) = \frac{1}{2.\tau \mathrm{Logn}\left(\frac{1+\alpha}{1-\alpha}\right)} \text{ (b)} \\ f_{min}(\,x_{max},\alpha) = \\ \frac{1}{\tau.\mathrm{Logn}\left(\frac{\left[((1-\alpha)x_{max})^2-((\alpha+1)E)^2\right]}{\left[((1-\alpha)x_{max})^2-((\alpha-1)E)^2\right]}\right)} \text{ (c)} \\ 0 < \alpha_1 < 1 \text{ (d)} \end{cases} \quad (20)$$

B. Optimization of the Digital IIR

The optimal digital IIR filter for DCM waves is designed using the *Least pth Norm method*. As a brief recall, let us consider a given ideal IIR filter with transfer function $F_p(\omega)$, and an unknown digital IIR to be determined, with M zeros and N poles, associated with the transfer function,

$$F(\omega, a, b) = \frac{B(\omega,b)}{A(\omega,a)} = \frac{\sum_{n=0}^{M} b(n)\, e^{-j\omega n}}{1-\sum_{k=0}^{N} a(n)\, e^{-j\omega n}} \quad (21)$$

where A(ω) and B(ω) are Fourier transforms of the numerator and denominator polynomial coefficients respectively, with real values b(n) and a(n) corresponding to the unknown sets of coefficients (22).

$$a = [b(0), b(1), \ldots b(M\text{-}1)],\ b = [a(1), a(2), \ldots, a(N)] \quad (22)$$

Then, the p^{th} Holder norm of the overall frequency response error between F(ω) and $F_0(z)$, is given by (23).

$$\|E(K, a, b)\|_p = \left(\left| \sum_{k=0}^{K-1} W_k \left(|F(\omega_k, a, b)| - |F_p(\omega_k)|^p \right) \right| \right)^{1/p} \quad (23)$$

Hence, the Digital IIR filter optimization problem is formulated as:

$$\begin{cases} \mathrm{Min}_{a,b}\left(\|E(K, a, b)\|_p \right) \text{ with} \\ b = [b(0)\ b(1)\ \ldots\ b(N)] \\ a = [a(1)\ a(2)\ \ldots\ a(N)] \end{cases} \quad (24)$$

In fact, (24) is an unconstrained convex minimization problem for a suitable choice of p. Because of the convexity property, the existence of the optimal set of parameters a and b is predictable. As it will be seen in Section IV, a reweighted least square Newton method is usually implemented in advanced numerical analysis such as MATLAB optimization toolbox, for the sake of rapid resolution of (20) and (24).

IV. Case Study of the Prototyping oDCM-Based ADC System

The parameters of the prototyping DCM-based DAC system considered in this section are: Modulating bandwidth f_m = 2 KHz, basic DCM frequency $f_m(0)$ =2 KHz, oversampling sampling frequency f_s = 25 MHz (i.e. sampling period T_m = 40 ns equivalently), E=9 volts, and $\tau = RC$ = 0.000115510618677s.

A. Optimal DCM

The nonlinear optimization problem (19) is solved successfully in practice using the *fmincon* tool available in MATLAB optimization toolbox. The optimal solution obtained is,

$$\alpha^* = 0.012366816265686,$$

and the graph of the corresponding absolute linearization error $|\varepsilon^*(x)|$ is shown in Fig. 4 [9], where it is apparent that the optimal error converges uniformly to zero in the whole modulating range [-3 V 3 V] .

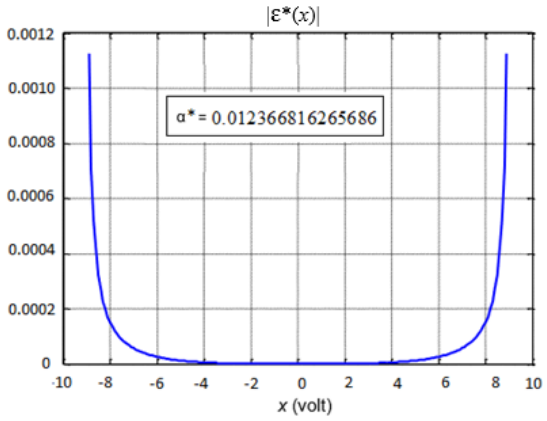

Fig. 4 Graph of the optimal absolute linearization error [9]

B. Optimal Second Order IIR Filter

Three relevant reasoning steps are useful for the design of the optimal IIR filter.

1) *Un-optimal second order IIR filter*: In order to appreciate the impact factor of the Least p^{th} norm used in this paper, the frequency points of the ideal H(ω) are selected from

the shape of the discrete version of a *second order filter* used in [9]. Its continuous transfer $F_0(s)$ and discrete transfer function $F_0(z)$ (under Tustin's discretization method), are given by (25) and (26) respectively.

$$F_0(s) = \frac{10300}{0.0000484s^2+0.2684s+10000} \quad (25)$$

$$F_0(z) = \frac{b2\,z^2 + b1\,z + b0}{z^2+a1\,z + a0} \quad (26)$$

with
$b2=8.263545624646787e^{-08}$
$b1=1.652709124929357e-07$
$b0=8.263545624646787e-08$
$a1=-1.999777875893610$
$a0=0.9997782064354348$

2) *Design of optimal second order IIR filter*: The second optimization scheme is modelled by (24), and the cost function $\|E(K,a,b)\|_p$ is defined according to (23). The resulting optimal solution has been computed successfully using the *iirlpnorm* tool available in MATLAB optimization toolbox. A sample of frequency response shapes of filters involved at the design state is plotted in Fig. 5, where the optimality of the design is quite apparent.

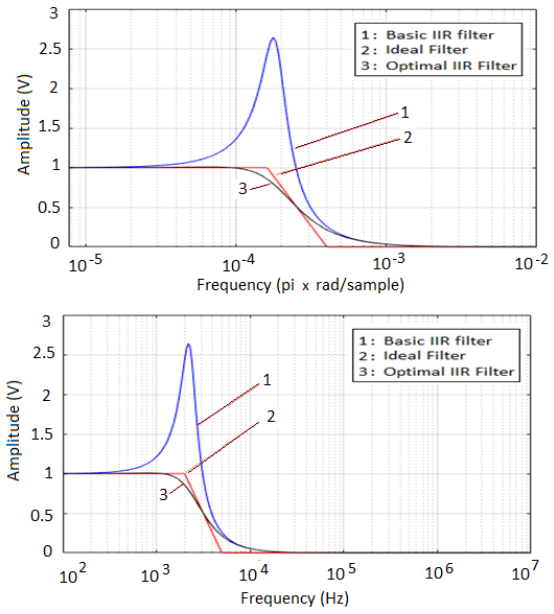

Fig. 5 Design of the optimal digital IIR filter from the response frequency of an un-optimal filter tool

Following this design, the discrete transfer function of the optimal IIR filter obtained is given by:

$$F(z) = \frac{b2\,z^2 + b1\,z + b0}{z^2+a1\,z + a0} \quad (27)$$

with
$b2= 8.530034325497877e-08$
$b1=1.706006865099575e-07$
$b0= 8.530034325497877e-08$
$a1=-1.999226624437879$
$a0=0.9992269656392521$

3) *Optimal resolution (number of bits)*: The optimal resolution offered by the ODCM-based ADC output is predicted by the following theorem

Theorem 4. Convexity of m(α*, x): The resolution function m(α*, *x*) in (12) is a convex function of *x*.

Following [9], [10], the proof of Theorem 4 becomes straightforward since,

$$\frac{\partial m\,(x,\alpha^*)}{\partial x} = \frac{8\,\alpha^* E^2\,x\,(1/T_m(x,\alpha^*))}{(1-\alpha^*)^2\,(x^2-E^2)^2} \quad (28)$$

Then, it is clear from (28) that the minimum of m(α*, *x*) in (12) is achieved at $x = 0$, and is given by,

$$m_{min}(0,\,\alpha^*) = \log_2\left(2\,\tau\,f_{ech}\,\mathrm{Log_n}\left(\frac{1+\alpha^*}{1-,\alpha^*}\right)\right) \quad (29)$$

C. Virtual Simulation of the ODCM-Based ADC System

Following (2), the ODCM-based ADC system, designed in depth in this section, has been implemented in Simulink framework as shown in the virtual model (see Fig. 6). It consists of a visual model of the optimal DCM block as shown in Fig. 6 (a), corresponding to the first order dynamic model (2), and a discrete transfer function F(z) of the optimal second order digital IIR filter.

The simulation required for performance evaluation of the overall prototyping ODCM-based ADC, is conducted over a sufficiently wide range of frequency including the modulating bandwidth of 3 KHz. In addition, a sample of detailed result related to a sine modulating input (1 KHz, 1 Vpp) is presented in Fig. 7, whereas all results obtained under variable modulating frequencies are summarized in Fig. 8.

Fig. 7 (a) shows that the ADC input and output signals have identical frequencies, with a sliding effect observed between their amplitudes. It might be cancelled if a third order digital IIR filter is used. In Fig. 7 (b) where the power spectrum of the optimal ADC output is plotted using MATLAB *iirlpnrom* tool, the resulting SFDR incurred is 56.74 dB. The same power spectrum might be used also to compute other standard performance indicators, e.g. SINAD. Finally, a summary of simulation results obtained are presented in Fig. 8.

The results presented here show that, the proposed pioneering ODCM-based ADC offers high performance within 3 KHz of modulating bandwidth, e.g., 57 dBc of SINAD (SIgnal-to-Noise and Distortion), 58 dB of SFDR (Spurious Free Dynamic Range) and -80 dBc of THD, while maintaining a minimum ADC resolution of 10 bits.

The high level of predicted performance obtained from virtual simulation of a prototyping system, is a great challenge an oversampling ADC topology, consisting of a piece of ODCM circuit with impressive properties, and a single stage of optimal 2nd order digital decimation filter.

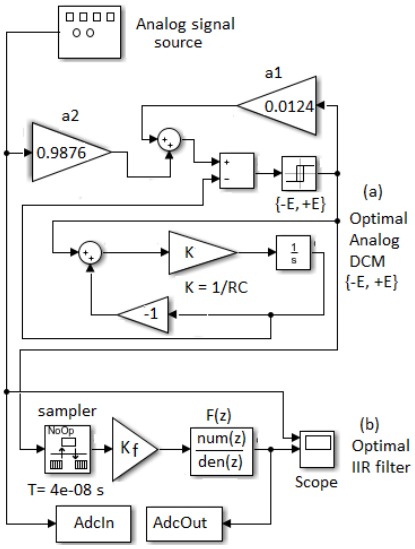

Fig. 6 Simulink model of the ODCM-based ADC system

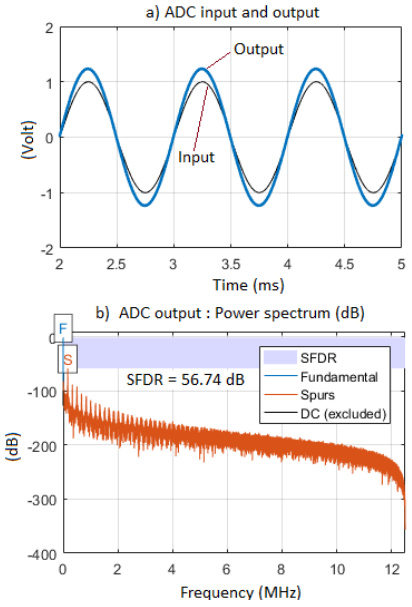

Fig. 7 Simulation of ODCM-based ADC for (1Kz, 1Vpp) input

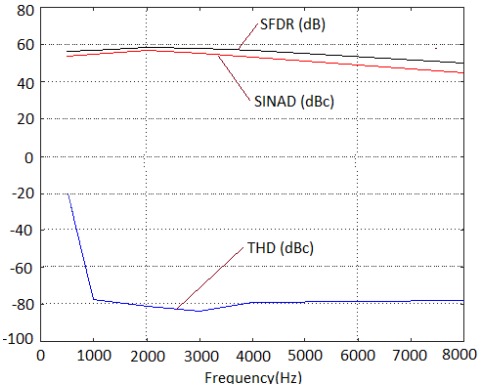

Fig. 8 Performance of the ODCM-Based ADC Output

V. Conclusion

Relevant morphological lemmas and theorems, followed by virtual simulation under MATLAB/Simulink frameworks, have been used in this paper, in order to show the feasibility and to check the optimality of ODCM-based ADC systems. The high performance offered under 3 HKz of modulating bandwidth, might become insufficient for ADC application areas with greedy ADC requirements. In such cases, it could be necessary to resort to either a greater sampling frequency or to increase the order of the digital IIR filter. Fortunately, the proposed optimization scheme structurally remains unchanged under these further improvements. It will be appreciable also to build a real prototype of the ODCM-based ADC, for FPGA-based instrumentations systems in industrial electronics. These extensions and new issues will be the core of future research works.

References

[1] H. Inose, Y. Yasuda and J. Marakami, "A telemetering system by code modulation, delta-sigma modulation," IRE Trans. on Space, Electronics and Telemetry, SET-8, pp. 204-209, Sept 1962.

[2] N. Doley and A. Kornfeld, "Comparison of Sigma-Delta converter circuit architectures in digital CMOS technology", Journal of circuits, systems ans computers", vol. 14, No 3, pp. 515-532, © World scientific publishing company, 2005.

[3] J. Mbihi, B. Ndjali, and M. Mbouenda, "Modelling and simulations of a class of duty cycle modulators for industrial instrumentation," *Iranian J. Electr. Comput. Eng.*, vol. 4, no. 2, pp. 121–128, 2005.

[4] Mbihi, J., Ndjali Beng, F., Kom, M., and Nneme Nneme, L. "*A novel analog-to-digital conversion technique using nonlinear duty-cycle modulation*", International Journal of electronics and computer science engineering, 1(3), 2012, pp. 818-825.

[5] I. Mbihi, L. Nneme Nneme, "A Multi-Channel Analog-To-Digital Conversion Technique Using Parallel Duty-Cycle Modulation". *International Journal of Electronics and Computer Science Engineering*. 2012; 1(3):826–833p.

[6] Nneme Nneme L., Mbihi J. "Modeling and Simulation of a New Duty–Cycle Modulation Scheme for Signal Transmission System", *American Journal of Electrical and Electronic Engineering (AJEEE)*.2014;2(3):82.

[7] Moffo Lonla B., Jean Mbihi, Leandre Nneme Nneme, "Low Cost and High Quality Duty–Cycle Modulation Scheme and Applications". *International Journal of Electrical, Computer, Energetic, Electronic and communication Engineering*. 2014; 8(3):82–88p.

[8] Moffo Lonla B., Mbihi J., Nneme Nneme L., Kom M. "A Novel Digital–to–Analog Conversion Technique using Duty-Cycle Modulation". *International Journal of Circuits, Systems and Signal processing*. 2013; 7(1):42–49p –87p.

[9] Moffo Lonla B., Mbihi J. A, "Nouvelle technique de coversion N/A des signaux par modulation numérique en rapport cyclique et applications en instrumentation virtuelle", Ph/D thesis, ENSET, University of Douala, July 2016.

[10] Moffo Lonla B., Mbihi J. A. "Novel Digital Duty–Cycle Modulation Scheme for FPGA-Based Digital-to-Analog Conversion," *IEEE Transaction on circuits and system II*. 2015; 62(6):543–547p.

G. Sonfack is born in 1983 in Fogo Togo at Dschang, Cameroon. She obtained the *Master Research* degree in electrical and automation engineering in 2015, at the EEAT (Electrical, Electronic, Automation and Telecoms) research laboratory of the *PhD Training Program* in Engineering Science of the University of Douala, Cameroun. She obtained also the *Master of Technical Education* in electrical engineering in 2012 at ENSET of Douala.

She is Head of Electrical Department of Advanced Vocational Training Center of Douala, Cameroon. She is also a graduate student in the PhD Training Program in Electronics and communication of the Faculty of Science

of the University of Dschang, Cameroon. Her PhD research topic deals with *Optimal Duty-Cycle Modulation Policies for FPGA-Based ADC Systems*.

J. Mbihi was born at Dschang, Cameroon, in 1960. He obtained *PhD* and *MscA* degrees in electrical and computer engineering at *Ecole Polytechnique of Montrea*l, Quebec (Canada), in 1999 and 1992 respectively. He obtained also the *Advanced Study Degree* in 1987 at ENSET of the University of Tunis, Tunisia. He received the *Master degree for Technical Education* in 1985 at ENSET of the University of Douala, Cameroon. He is owner of a patent (Nº 9048, PV 58580, March 31 1991), on *Multi-caliber battery charger* with *Automatic stopping and calibrating*, from *African Organization of Intellectual Rights,* Yaoundé, Cameroon.

He created the IIA (Industrial Informatics and Automation) Research team in 2001 at ENSET of Douala, and became since 2004 he deputy Coordinator of the Research Laboratory in EEAT (Electrical, Electronic, Telecoms and Automation) engineering, of the PhD Training Program in Engineering Science of the University of Douala. He is Head of the department of Textile and Fashion Industry at ENSET of Douala since 2004. He is also author of a first book "*Informatique et Automation – Automatisme programmable contrôlés par ordinateur*", 358 pages, © Publibook Editions (Paris, 2006), and main co-author of a second book "*Informatique Industrielle – Instrumentation virtuelle assistée par ordinateur*", 248 pages, © Ellipses editions (Paris, 2012). He is also author and co-author of a great number of relevant articles published in international scientific societies including IEEE Transactions and World Academy of Science, Engineering and Technology. His current research interest is focused on DCM-Based instrumentation and remote control Technology, for deterministic and stochastic dynamic systems.

Pr Mbihi is member of many scientific societies including IAENG (*International Association of Engineers*), and *RAIFFET* (*Réseau Africain des Institutions de Formation de Formateur de l'Enseignement Technique*). He is indexed in leading scientific communication networks including *Research Gate*.

B. Lonla Moffo was born in Mbouda, Cameroun, in 1978. He received the PhD and Master Research degrees in Electrical and Automation engineering in 2011 and 2016 respectively, from the EEAT research laboratory of the *PhD Training Program* in Engineering Science of the University of Douala, Cameroun He received also the *Master of Technical Education* in electrical engineering in 2007 at ENSET of Douala.

He served as Assistant Lecturer at *College of Technology* of the university of Buea, Cameroon, during 2011-2013. Then, he was promoted in November 2016 as senior Lecturer in the department of Computer Science of HTTC (Higher Technical Teachers' College) for Technical Education of the university of Buea, where he is Head of the Department of Computer Science since 2014.

He is also an active member of the research team in *Industrial Computer Science and Automation*, created at ENSET of the University of Douala since 2001. He is coauthor of many articles published in international scientific societies including IEEE Transactions and World Academy of Science, Engineering and Technology.

His current research interests include digital DCM-Based instrumentation technologies, and automation.